Seawater desalination with solar-energy-integrated vacuum membrane distillation system

Fang Wang, Shixuan Wang, Jin Li, Dongsheng Xia and Jianshe Liu

ABSTRACT

This study designed and tested a novel type of solar-energy-integrated vacuum membrane distillation (VMD) system for seawater desalination under actual environmental conditions in Wuhan, China. The system consists of eight parts: a seawater tank, solar collector, solar cooker, inclined VMD evaporator, circulating water vacuum pump, heat exchanger, fresh water tank, and brine tank. Natural seawater was used as feed and a hydrophobic hollow-fiber membrane module was used to improve seawater desalination. The experiment was conducted during a typical summer day. Results showed that when the highest ambient temperature was 33 °C, the maximum value of the average solar intensity was 1,080 W/m^2. The system was able to generate 36 kg (per m^2 membrane module) distilled fresh water during 1 day (7:00 am until 6:00 pm), the retention rate was between 99.67 and 99.987%, and electrical conductivity was between 0.00276 and 0.0673 mS/cm. The average salt rejection was over 90%. The proposed VMD system shows favorable potential application in desalination of brackish waters or high-salt wastewater treatment, as well.

Key words | desalination, hollow-fiber membrane, seawater, solar energy, vacuum membrane distillation

Fang Wang
Jianshe Liu (corresponding author)
State Environmental Protection Engineering Center for Pollution Treatment and Control in Textile Industry,
College of Environmental Science and Engineering,
Donghua University,
Shanghai 201620,
China
E-mail: *liujianshe@dhu.edu.cn*

Shixuan Wang
Jin Li
Dongsheng Xia
Engineering Research Center for Clean Production of Textile Dyeing and Printing, Ministry of Education,
Wuhan Textile University,
Wuhan 430200,
China

INTRODUCTION

Currently, there is an urgent need for pure, clean drinking water in many countries across the globe. Water shortages have become a major environmental issue that is further impacted by global warming. Brackish water sources are not potable due to the content of dissolved salts and harmful bacteria. Similarly, many coastal areas have abundant seawater, but no safe drinking water. Distillation can be used to purify water supply, and is one of many techniques for desalinating seawater (Aybar *et al.* 2005). With the rapid increase of the world population, desalination is increasingly considered to be necessary and feasible. By 2025, about 70% of the world's population will face water shortage problems (Li *et al.* 2013). Seawater desalination is recognized as one of mankind's earliest ways of water treatment, and it provides fresh water for many communities and manufacturers. It plays an important role in economic development in many developing countries, especially in water shortage countries such as Pacific Asia, Africa and Middle East countries (Shatat *et al.* 2013).

There have been several recent developments in water desalination techniques, including membrane distillation (MD). MD is considered a valid alternative to traditional desalination techniques such as coupling to reverse osmosis (RO), also called 'integrated membrane systems', or multi-stage flash vaporization (MSFV). MD is less influenced by osmotic pressure than RO, and consumes less energy than MSFV. According to which pattern is used to condense volatile components in the permeate side of the system, MD can be classified into the following four structures: (i) direct contact MD (Gryta & Barancewicz 2010; Teoh *et al.* 2011; Yu

doi: 10.2166/wrd.2016.207

et al. 2011); (ii) air gap MD (Banat et al. 1999; Yao et al. 2013); (iii) sweeping gas MD (Rivier et al. 2002; Cojocaru & Khayet 2011); and (iv) vacuum MD (VMD) (Porter 1972; Bandini et al. 1992, 1997; Sarti et al. 1993; Bandini & Sarti 1999; Zhao et al. 2011). MD can be applied in many fields. A previous study confirmed that benzene and heavy metals can be removed from water by MD for environmental applications (El-Bourawi et al. 2006; Khayet 2011; Susanto 2011; Alkhudhiri et al. 2012), for example, and another suggested that MD can be applied successfully in the food industry, where concentrated fruit juices and sugar solutions can be prepared with better flavor and color using MD with a low operating temperature (Calabro et al. 1994). Research has also shown that high-temperature MD can be applied successfully in the medical field to sterilize biological fluids (Sakai et al. 1988).

Although MD has many attractive features, such as the possibility of coupling to low-grade sources of energy, it has not yet been commercialized for large-scale desalination plants due to technical problems involving low flux and membrane wetting. These, and other design drawbacks, are expected to be overcome because a wealth of research has gone into developing MD components and processes, including membranes (Sakai et al. 1988; Calabro et al. 1994; Lawson & Lloyd 1997; Susanto 2011). Researchers have highlighted the possibility that MD can be integrated with renewable and low-grade energy sources such as solar and wind, which offers promising techniques (Cabassud & Wirth 2003; Xu et al. 2006). Solar energy, low-grade waste heat, and geothermal energy represent favorable alternative sources. Koschikowski et al. (2003) showed a solar thermal-driven spiral wound polytetrafluoroethylene MD module was used to obtain potable water from brackish water and seawater in another study. Aybar (2006) reported an inclined solar water distillation system can generate 3.5–5.4 kg (per m^2 absorber plate area) distilled water during a normal summer day in North Cyprus. Asadi et al. (2013) have shown that solar still systems can remove inorganic, organic, and bacteriological contaminants quite effectively; a test system proved extremely successful in removing such contaminants from wastewater. Kaya et al. (2015) developed a single NF (nanofiltration) and SWRO (seawater reverse osmosis) membranes, as well as an NF + SWRO integrated system, which were tested in terms of permeate quality and quantity using natural seawater. The NF + SWRO integrated system proved an effective pretreatment for seawater desalination.

There have been relatively few studies on solar-energy-integrated VMD systems for seawater desalination. The present study designed and built a new type of solar-energy-integrated VMD system for seawater desalination. The objective of this study was to investigate the feasibility of the proposed system to produce fresh water from natural seawater during a typical summer day in Wuhan, China. Changes in ambient temperature and solar intensity with time were measured, as well as temperature changes of the feed seawater, seawater in the solar collector, seawater in the solar cooker, glass lid, evaporator, vapor, fresh water, and strong brine with time. The quality and quantity of fresh water output from the system were also tested. The results altogether confirmed the feasibility of producing fresh water with solar-energy-integrated VMD systems.

MATERIALS AND METHODS

Materials

Shade type hydrophobic hollow-fiber membrane module was from China Hangzhou Haotian Membrane Separation Technology Co., Ltd. The membrane component parameters are reported in Table 1. Seawater was taken from the South China Sea. The characteristics of natural seawater are listed in Table 2.

Table 1 | Membrane component parameters

Parameter	Value or definition
Membrane material	Polypropylene
Membrane inner diameter (μm)	250–300
Membrane outer diameter (μm)	350–400
Membrane pore size (μm)	0.1–0.2
Wall thickness (μm)	40–50
Porosity (%)	40–50
Tensile strength (Mpa)	120
pH	0–14
Membrane area (m^2)	2
Dimensions of membrane module (mm): (length × width)	810 × 520

Table 2 | Characteristics of natural seawater

Parameter	Unit	Value
pH	–	7.88
Temperature	°C	20
Salinity	psu	15
Turbidity	NTU	10.8
EC	mS/cm	20.7
SS	(mg/L)	4.0
TDS	(mg/L)	10,310
TOC	(mg/L)	4.38
Total bacterial count	CFU/mL	24,100
COD	(mg/L)	16.8
Na^+	(mg/L)	4,316.5
Mg^{2+}	(mg/L)	504.3
Ca^{2+}	(mg/L)	204.1
K^+	(mg/L)	175.6
Sr^{2+}	(mg/L)	3.47
Cl^-	(mg/L)	7,795.5
SO_4^2	(mg/L)	1,115.8
Br	(mg/L)	38.1
F^-	(mg/L)	0.54

psu, practical salinity units; NTU, nephelometric turbidity unit; ms/cm, milli Siemens per cm; CFU, colony forming units.

Experimental system descriptions

A schematic diagram of the system is shown in Figure 1, a simplified schematic diagram is shown in Figure 2, and a photo of the system is shown in Figure 3. A miniature, pilot-scale seawater desalination system was installed on the Wuhan Textile University laboratory building roof (Wuhan City, Hubei Province, China). The system module characteristics are listed in Table 3. The complete system consists of a seawater tank, solar collector, solar cooker, inclined VMD evaporator, circulating water vacuum pump, heat exchanger, fresh water tank, and brine tank. The system is equipped with a rotating base that can be adjusted manually according to the position of the sun, allowing the system to fully receive the available solar radiation. Thermometers were installed on the inlet and outlet of all pipes in the system to gather data for subsequent analysis.

As shown in Figures 1 and 2, the operation process of the system includes the following steps. First, natural seawater is put into the seawater tank and enters the heat exchanger via the first peristaltic pump, where natural seawater is preheated by vapor. Next, seawater enters the solar collector via the second peristaltic pump, where it is heated. Seawater then flows into the solar hot water tank and is heated again in the solar cooker. After being heated a total of three times, the seawater enters the VMD evaporator and flows down through the hole in the support plate; at this time, the membrane module is hung above the support plate, and then the hot seawater evaporates slowly into vapor. The vapor passes through the membrane hole from the hot side of the membrane module into the cold side of the membrane module, where the circulating water vacuum pump reduces the pressure. The vapor is then pumped into the heat exchanger where heat exchange with natural seawater takes place, thus condensing the vapor as fresh water. The strong brine left after desalination is recycled into the seawater tank and mixed with natural seawater to obtain a higher feed temperature, but in a practical application, the strong brine goes directly into the ocean.

Analytical methods

System performance was mainly tested in terms of fresh water quality and quantity. The quantity of fresh water was checked according to membrane flux and retention rate, and the quality of fresh water (and seawater) was analyzed according to salinity, conductivity, temperature measurements, and total dissolved solids (TDS) content, determined using a portable HACH Sension5 conductivity meter. The pH values were measured with a digital pH meter (Sartorius PB-10). Suspended solids (SS) content was measured according to the weight method, and chemical oxygen demand (COD) was determined by the basic potassium permanganate method. Total organic carbon (TOC) was determined using a TOC analyzer (Multi N/C2100) and the total number of bacteria was counted by plate count method. The Na^+, Mg^{2+}, Ca^{2+}, K^+, and Sr^{2+} ion concentrations were each measured with an atomic absorption spectrophotometer (GBC AVANTA M Model). The Cl^-, SO_4^{2-}, Br^-, and F^- ion levels were determined with ion chromatography equipment (ICS 900 model).

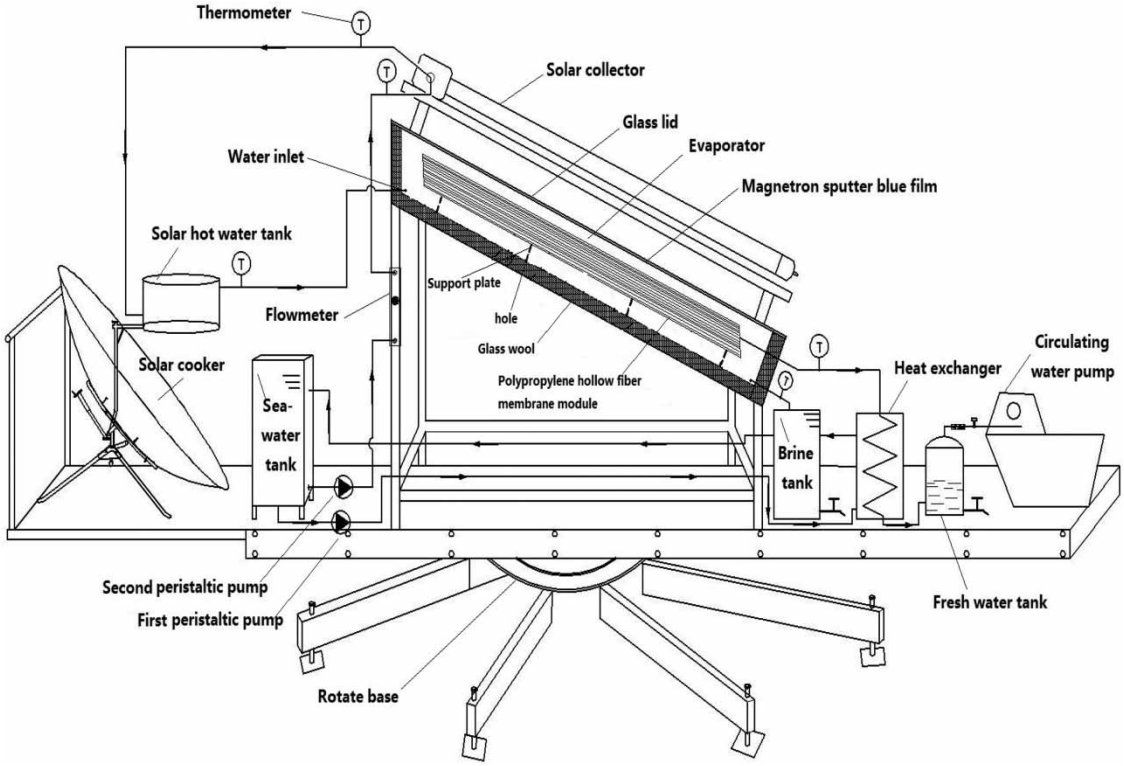

Figure 1 | Schematic diagram of test system.

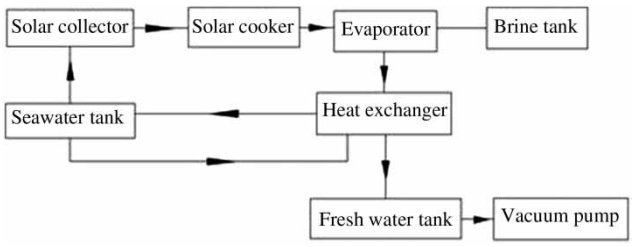

Figure 2 | Simplified schematic diagram.

Calculations

Membrane flux (J) was the amount of liquid produced per unit area of a membrane surface per unit of time. Retention rate (η) was the percentage of dissolved solids intercepted by the membrane that occupied the total quantity of the solute in the solution. Due to the ratio of NaCl concentration and its conductivity being approximate to constant, when the retention rate was calculated, conductivity was used instead of concentration. They were calculated using the following equations:

Figure 3 | Photo of test system.

$$J\left(\frac{\mathrm{kg}}{\mathrm{m}^2 \cdot \mathrm{h}}\right) = \frac{W}{S * \mathrm{t}} \tag{1}$$

Table 3 | Characteristics of system module

Main device	Parameter	Value or definition
Solar collector		
	Material of solar collector	All-glass vacuum tube
	Number of tubes	12
	Heat absorption efficiency ($W/cm^2 \cdot h$)	850
	Effective heat absorbing area (m^2)	1.62
Evaporator		
	Material of evaporator	Stainless steel
	Material of glass lid	Hollow toughened glass
	Heat-absorbing aluminum	Magnetron sputter blue film
	Glass angle (°)	30
	Dimensions of evaporator	
	Length (m)	1.90
	Width (m)	0.95
	Height (m)	0.3
	Water inlet	Top of evaporator
	Material of the support plate	Stainless steel
	No. of the support plate	4
	Height of the support plate (cm)	5
	Diameter of the hole (cm)	2.5
	No. of the hole (each support plate)	3
Solar cooker		
	Material of solar cooker	Carbon steel plate
	Stove diameter (m)	1.80
	Focal length (m)	0.68
	Focal spot temperature (°C)	1,100
	Effective heat absorbing area (m^2)	2.20
	Concentration ratio	8/45
	Sunny day power (W)	2,000
Seawater tank		
	Material of the seawater tank	Stainless steel
	Dimensions of seawater tank	
	Length (m)	0.60
	Width (m)	0.30
	Height (m)	0.30
Solar hot water tank		
	Material of solar hot water tank	Stainless steel cylinder, black
	Dimensions of solar hot water tank	
	Diameter (m)	0.32
	Height (m)	0.15
Heat exchanger		
	Dimensions of heat exchanger	
	Length (m)	0.20
	Width (m)	0.20
	Height (m)	0.40
	S-type heat exchanger coil (m)	9.42
Brine tank		
	Dimensions of brine tank	
	Length (m)	0.20
	Width (m)	0.20
	Height (m)	0.40

(*continued*)

Table 3 | continued

Main device	Parameter	Value or definition
Vacuum pump		
	Power (W)	180
	Voltage/frequency (V/Hz)	220/5
	Flow (L/min)	60
	Maximum vacuum degree (Mpa)	0.098
Peristaltic pump		
	Power (W)	200
	Range of speed	60–600 rpm
Rotate base		
	Dimensions of rotating base	
	Length (m)	5
	Width (m)	1.2
	Material of rotating base	Steel

$$\eta(\%) = \frac{(\rho_h - \rho_c)}{\rho_h} \quad (2)$$

where W, S, t, ρ_h, and ρ_c are fresh water quantity (kg), the effective area of the membrane (m^2), operation time (h), the conductivity of natural seawater (mS/cm), and the conductivity of fresh water (mS/cm), respectively.

RESULTS AND DISCUSSION

The system operated from 7:00 am to 6:00 pm on August 22nd, 2015, a day which had normal weather and good air quality. When the system is running, the quantity of feed seawater was set to 220 L, seawater inlet flow was set to 20 L/h, and the vacuum degree of the cold side was set to 0.095 Mpa. All tests were performed and repeated in the same environment.

Changes of ambient temperature and solar radiation intensity

Figure 4 shows the changes in ambient temperature and hourly average of solar radiation intensity with time. Over the course of the operation time, both ambient temperature and solar radiation intensity with time increased at first, and then decreased. Meteorological data showed that the average ambient temperature was between 26 and 33 °C, and that the average solar radiation intensity was between 744 and 1,080 W/m^2. Solar intensity increased as the ambient temperature rose; the two values form a parabola when plotted. The highest ambient temperature, 33 °C, was recorded at 2:00 pm; solar radiation intensity reached its peak value of 1,080 W/m^2 at the same time.

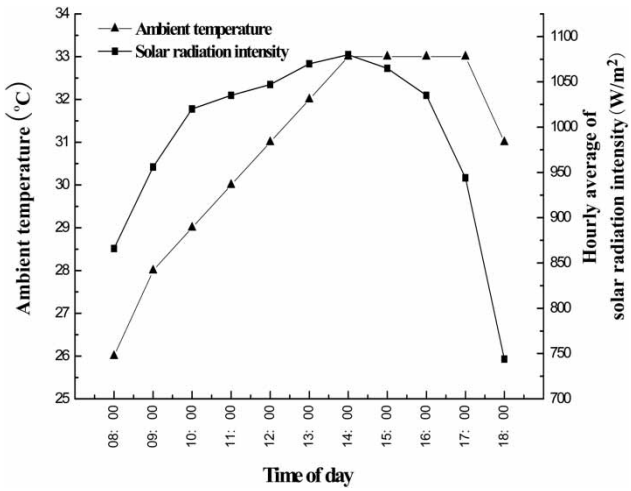

Figure 4 | Ambient temperature and hourly average of solar radiation intensity with time.

Temperature changes of feed seawater, solar collector seawater, solar cooker seawater, glass lid, evaporator, vapor, fresh water, and strong brine

Temperature changes in the hourly average of the feed seawater, the seawater in the solar collector, and the seawater in

the solar cooker, as well as the glass lid, evaporator, vapor, fresh water, and strong brine with time were measured as shown in Figure 5. The temperature of feed seawater rose continually throughout the operation process as strong brine was recycled into the seawater tank and mixed with seawater, and as feed seawater was heated by the vapor in the heat exchanger. Throughout the test day, the seawater temperature in the solar collector and solar cooker first increased while solar radiation intensity increased, then decreased as solar radiation intensity decreased. The temperature of the evaporator was lower than that of the solar cooker, naturally, because seawater temperature increased in the cooker then lost heat during evaporation. Fresh water temperature was lower than vapor temperature, because vapor in the heat exchanger was condensed by feed seawater until becoming fresh water. The above temperature measurements altogether prove that it is feasible to heat seawater by using a solar collector coupled with a solar cooker.

Change of membrane flux

A hydrophobic, hollow-fiber membrane module was employed in this study. The performance of the system was evaluated in terms of both the quality and quantity of fresh water produced. The quantity of fresh water was checked by membrane flux; changes in membrane flux over time are shown in Figure 6. The hydrophobic, hollow-fiber membrane exhibited different fresh water production outputs and membrane flux values at different times during the test process. At 2:00 pm, at 0.095 Mpa vacuum degree on the cold side, the maximum value for membrane flux was 7.88 kg/m^{2}h. As seawater temperature increased, steam partial pressure of the membrane on the hot side plus the driving force of the steam through the membrane increased, thus causing increased membrane flux. As mentioned above, at 2:00 pm, the seawater temperature in the solar cooker also reached its maximum value.

Changes of fresh water electrical conductivity and retention rate

Figure 7 shows the measured changes in fresh water electrical conductivity (EC) and retention rate over time during the test period. The retention rate was between 99.67 and 99.987%, and the EC was between 0.00276 and 0.0673 mS/cm, confirming that the hydrophobic, polypropylene hollow-fiber membrane module provided favorable separation performance to the experiment. At 2:00 pm, when the seawater temperature of the evaporator reached its maximum value, the retention rate reduced slightly; elevated feed seawater temperatures caused thermal motion to increase in the NaCl solution ions, thereby forcing an increased amount of gas phase ions through the membrane module.

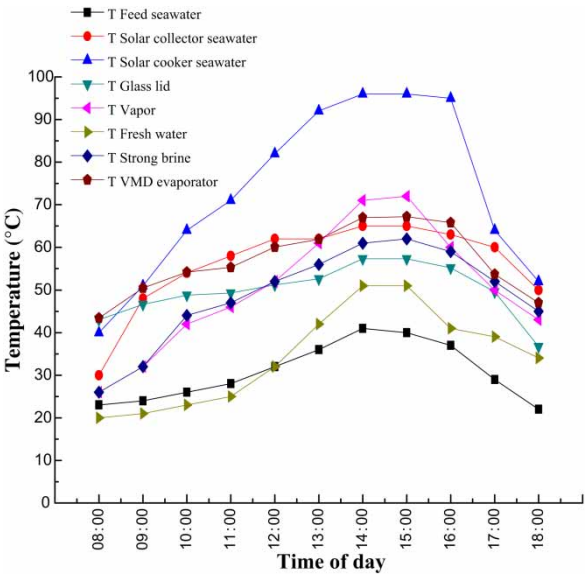

Figure 5 | Temperature changes of feed seawater, solar collector seawater, solar cooker seawater, glass lid, vapor, fresh water, strong brine, and evaporator with time.

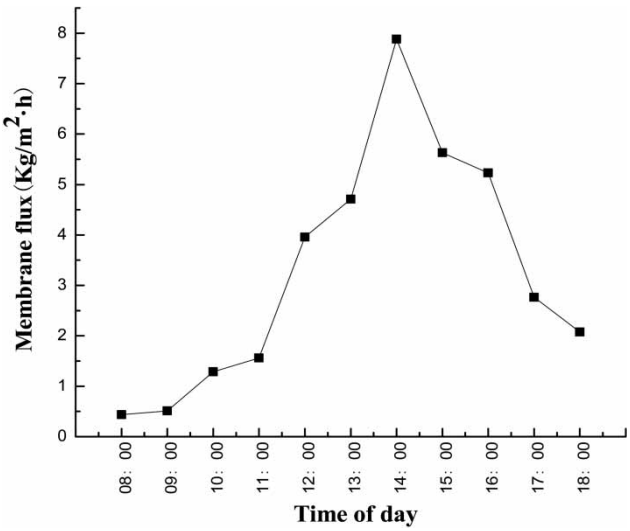

Figure 6 | Membrane flux changes over time.

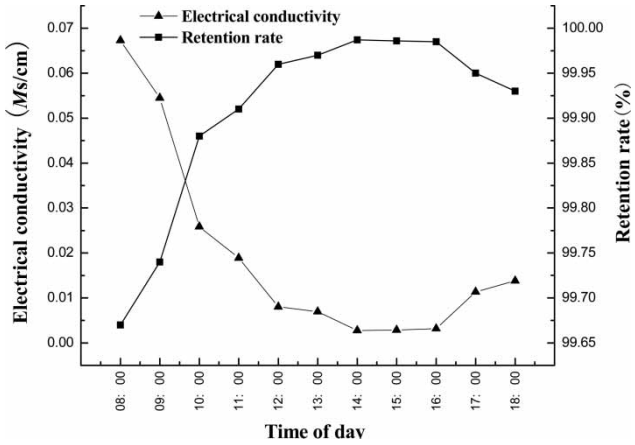

Figure 7 | Fresh water EC and retention rate changes with time.

Characteristics of fresh water obtained by the system

Table 4 lists the characteristics of fresh water obtained by the test system. The average removal rates of SS, TDS, TOC, COD, Na^+, Mg^{2+}, Ca^{2+}, K^+, Sr^{2+}, Cl^-, SO_4^{2-} and F^- were 50–70%, 99.68–99.99%, 68–94%, 97.56–97.86%, 99.942–99.996%, 99.677–99.996%, 97.09–99.86%, 99.47–99.91%, over 96.83%, 99.95–99.99%, 99.68–99.95%, and above 93%, respectively. In the literature, Kaya *et al.* (2015) also showed a similar rejection value by NF90 (30 bar) + SW30–RO (40 bar) combination; their average removal rates of TDS, Na^+, Mg^{2+}, Ca^{2+}, K^+, Cl^- and SO_4^{2-} were 98.89%, 98.94%, over 99.991%, 99.43%, 99.02%, 99.03%, and over 99.994%. These results altogether confirm that the test system desalinated seawater very effectively.

Table 4 | Characteristics of fresh water

Parameter	Unit	Value (min–max)
pH	–	7.57–7.64
Temperature	°C	27.4–27.5
Salinity	Psu	0
Turbidity	NTU	0.17–0.23
EC	mS/cm	0.00276–0.0673
SS	(mg/L)	1.2–2.0
TDS	(mg/L)	1.2–33.4
TOC	(mg/L)	0.28–1.39
Total bacterial count	CFU/mL	1–16
COD	(mg/L)	0.36–0.41
Na^+	(mg/L)	0.19–2.50
Mg^{2+}	(mg/L)	0.02–1.63
Ca^{2+}	(mg/L)	0.28–5.94
K^+	(mg/L)	0.15–0.93
Sr^{2+}	(mg/L)	<0.11
Cl^-	(mg/L)	0.612–4.053
SO_4^{2-}	(mg/L)	0.608–3.598
Br^-	(mg/L)	Not detected
F^-	(mg/L)	<0.039

The design advantages of this device can be summarized according to three major aspects: (i) the rotating base, which can be manually adjusted to suit the sun's position and fully exploit all available solar energy radiation; (ii) the solar collector coupled with the solar cooker to build the solar energy heat system, in which seawater can be rapidly heated to obtain very high water flux; and (iii) the hydrophobic, polypropylene hollow-fiber membrane module used for water vapor separation, which ensures high-quality fresh water.

CONCLUSIONS

In this study, a new type of solar-energy-integrated VMD system for seawater desalination was designed and tested under actual environmental conditions in Wuhan, China. The aim of this study was to determine the feasibility of using solar-energy-integrated VMD to obtain fresh water from natural seawater during a typical day, and to test the performance of the system in terms of both the quality and quantity of fresh water produced. According to our experimental results, the solar collector and solar cooker showed favorable performance related to temperature, membrane flux increased as seawater temperature increased, and the system was able to generate 36 kg (per m^2 membrane module) distilled fresh water during the test day (7:00 am until 6:00 pm). The retention rate was between 99.67 and 99.987%, EC was between 0.00276 and 0.0673 mS/cm, and the average salt rejection was above 90%. These results altogether confirm that solar energy integrated with VMD is an appropriate and effective combination for seawater desalination systems.

ACKNOWLEDGEMENTS

The authors would like to acknowledge the financial support provided by the National 'Twelfth Five-Year' Plan

for Science & Technology Support of China (No. 2014BAC13B02) and the National Science Foundation of China (NSFC) (No. 21377023).

REFERENCES

Alkhudhiri, A., Darwish, N. & Hilal, N. 2012 Membrane distillation: a comprehensive review. *Desalination* **287**, 2–18.

Asadi, R. Z., Suja, F. & Ruslan, M. H. 2013 The application of a solar still in domestic and industrial wastewater treatment. *Solar Energy* **93**, 63–71.

Aybar, H. Ş. 2006 Mathematical modeling of an inclined solar water distillation system. *Desalination* **190** (1), 63–70.

Aybar, H. Ş., Egelioğlu, F. & Atikol, U. 2005 An experimental study on an inclined solar water distillation system. *Desalination* **180** (1), 285–289.

Banat, F. A., Al-Rub, F. A., Jumah, R. & Al-Shannag, M. 1999 Application of Stefan–Maxwell approach to azeotropic separation by membrane distillation. *Chemical Engineering Journal* **73** (1), 71–75.

Bandini, S. & Sarti, G. C. 1999 Heat and mass transport resistances in vacuum membrane distillation per drop. *AIChE Journal* **45** (7), 1422–1433.

Bandini, S., Gostoli, C. & Sarti, G. C. 1992 Separation efficiency in vacuum membrane distillation. *Journal of Membrane Science* **73** (2–3), 217–229.

Bandini, S., Saavedra, A. & Sarti, G. C. 1997 Vacuum membrane distillation: experiments and modeling. *AIChE Journal* **43** (2), 398–408.

Cabassud, C. & Wirth, D. 2003 Membrane distillation for water desalination: how to choose an appropriate membrane? *Desalination* **157** (1), 307–314.

Calabro, V., Jiao, B. L. & Drioli, E. 1994 Theoretical and experimental study on membrane distillation in the concentration of orange juice. *Industrial & Engineering Chemistry Research* **33** (7), 1803–1808.

Cojocaru, C. & Khayet, M. 2011 Sweeping gas membrane distillation of sucrose aqueous solutions: response surface modeling and optimization. *Separation and Purification Technology* **81** (1), 12–24.

El-Bourawi, M. S., Ding, Z., Ma, R. & Khayet, M. 2006 A framework for better understanding membrane distillation separation process. *Journal of Membrane Science* **285** (1), 4–29.

Gryta, M. & Barancewicz, M. 2010 Influence of morphology of PVDF capillary membranes on the performance of direct contact membrane distillation. *Journal of Membrane Science* **358** (1), 158–167.

Kaya, C., Sert, G., Kabay, N., Arda, M., Yüksel, M. & Egemen, Ö. 2015 Pre-treatment with nanofiltration (NF) in seawater desalination – Preliminary integrated membrane tests in Urla, Turkey. *Desalination* **369**, 10–17.

Khayet, M. 2011 Membranes and theoretical modeling of membrane distillation: a review. *Advances in Colloid and Interface Science* **164** (1), 56–88.

Koschikowski, J., Wieghaus, M. & Rommel, M. 2003 Solar thermal driven desalination plants based on membrane distillation. *Water Science and Technology: Water Supply* **3** (5–6), 49–55.

Lawson, K. W. & Lloyd, D. R. 1997 Membrane distillation. *Journal of Membrane Science* **124** (1), 1–25.

Li, C., Goswami, Y. & Stefanakos, E. 2013 Solar assisted sea water desalination: a review. *Renewable and Sustainable Energy Reviews* **19**, 136–163.

Porter, M. C. 1972 Concentration polarization with membrane ultrafiltration. *Industrial & Engineering Chemistry Product Research and Development* **11** (3), 234–248.

Rivier, C. A., García-Payo, M. C., Marison, I. W. & Von Stockar, U. 2002 Separation of binary mixtures by thermostatic sweeping gas membrane distillation: I. Theory and simulations. *Journal of Membrane Science* **201** (1), 1–16.

Sakai, K., Koyano, T., Muroi, T. & Tamura, M. 1988 Effects of temperature and concentration polarization on water vapour permeability for blood in membrane distillation. *The Chemical Engineering Journal* **38** (3), B33–B39.

Sarti, G. C., Gostoli, C. & Bandini, S. 1993 Extraction of organic components from aqueous streams by vacuum membrane distillation. *Journal of Membrane Science* **80** (1), 21–33.

Shatat, M., Worall, M. & Riffat, S. 2013 Opportunities for solar water desalination worldwide: review. *Sustainable Cities and Society* **9**, 67–80.

Susanto, H. 2011 Towards practical implementations of membrane distillation. *Chemical Engineering and Processing: Process Intensification* **50** (2), 139–150.

Teoh, M. M., Chung, T. S. & Yeo, Y. S. 2011 Dual-layer PVDF/PTFE composite hollow fibers with a thin macrovoid-free selective layer for water production via membrane distillation. *Chemical Engineering Journal* **171** (2), 684–691.

Xu, Y., Zhu, B. K. & Xu, Y. Y. 2006 Pilot test of vacuum membrane distillation for seawater desalination on a ship. *Desalination* **189** (1), 165–169.

Yao, K., Qin, Y., Yuan, Y., Liu, L., He, F. & Wu, Y. 2013 A continuous-effect membrane distillation process based on hollow fiber AGMD module with internal latent-heat recovery. *AIChE Journal* **59** (4), 1278–1297.

Yu, H., Yang, X., Wang, R. & Fane, A. G. 2011 Numerical simulation of heat and mass transfer in direct membrane distillation in a hollow fiber module with laminar flow. *Journal of Membrane Science* **384** (1), 107–116.

Zhao, Z. P., Zhu, C. Y., Liu, D. Z. & Liu, W. F. 2011 Concentration of ginseng extracts aqueous solution by vacuum membrane distillation 2. Theory analysis of critical operating conditions and experimental confirmation. *Desalination* **267** (2), 147–153.

First received 25 November 2015; accepted in revised form 1 February 2016. Available online 26 March 2016